Damage Localization in Reinforced Concrete Slab Using Acoustic Emission Technique

Soumyadip Das[1,2(✉)], Aloke Kumar Datta[1], Pijush Topdar[1], and Sanjay Sengupta[2]

[1] NIT Durgapur, Durgapur, India
soumyadipdas.kaka@gmail.com, {alokekumar.datta, pijush.topdar}@ce.nitdgp.ac.in
[2] Dr. B.C. Roy Engineering College, Durgapur, India
sanjay.sengupta@bcrec.ac.in

Abstract. Reinforced Concrete (RC) Pavement which is basically a reinforced concrete slab is becoming very popular in recent times due to its prolonged structural life. Like all the other types of RC structures, internal cracks are developed in RC pavement due to several reasons like external loads, shrinkage, thermal expansion, corrosion etc. Such cracks are detrimental to the overall health of the pavement structure. Available literature suggests that acoustic emission (AE) is a very effective technique used for structural health monitoring (SHM) for detection of damage in similar kinds of pavements in real-time. Due to the development of crack, sudden release of strain energy causes elastic waves which can be detected using AE sensors. The literature indicates that such AE waves can be used for determining the location of damage. The further review of the available literature indicates that analysis of the AE waveforms in the frequency domain using Fast Fourier Transform (FFT) or Short Time Fourier Transform (STFT) or in time frequency domain using wavelet transform is also being used by the researchers in the past for localizing the damage in thin metal and multi-layered composite plates. However, as per the present knowledge of the authors the applicability of wavelet transform of AE waves in localizing the damage in RC slabs is found to be absent in literature. In the current study, the authors have made an attempt to localize the damage in a prototype RC slab using the higher symmetric & anti-symmetric modes and group velocity of AE waves. The results obtained for localization is found to be promising using the procedure.

Keywords: Reinforced concrete slab · Acoustic emission · Structural health monitoring · Wavelet transform

1 Introduction

Reinforced concrete (RC) pavements are basically reinforced concrete slabs resting on the top surface of the subgrade. Load coming from vehicular traffic is transferred to the soil subgrade through the pavement. The repetition of load causes cracks in the RC pavement which eventually leads to permanent damage in the pavement. Besides other factors like shrinkage, thermal expansion, corrosion etc. also cause damage in the

J. A. Fonseca de Oliveira Correia et al. (Eds.): ASMA 2021, STIN 26, pp. 162–170, 2023.
https://doi.org/10.1007/978-3-031-05509-6_13

pavement structure. In order to maintain the road in serviceable condition, monitoring the overall structural health of the RC pavement has become a topic of considerable interest to designers and highway management departments in recent times. Such monitoring, popularly known as structural health monitoring (SHM), is a term that states a range of systems implemented on constructed facilities with the purpose of assisting and informing the condition of structures under gradual or sudden changes to their state of serviceability. Out of many available techniques of SHM, the technique of Acoustic Emission (AE) is an important one that is being used extensively from last decade of the 20th century (Sengupta 2015). This technique has the competency to detect the location of damage sources in structures in real-time.

In AE technique, when a crack is developed, sudden release of strain energy causes elastic waves which can be detected using AE sensors. The data captured by the sensors may be analyzed to locate the crack, which may be called as an AE source. For finding the exact location of AE source, which is termed as localization, various approaches or methods are available in literature (Panjsetooni et al. 2013; Naredpour et al. 2017). Out of these them, source localization by signal processing approach has become popular among researchers in last few decades (Ebrahimkhanloua and Salamonea 2017). Frequency response of AE waveform; which are basically the time-dependent displacement responses, obtained through different mathematical techniques like fast Fourier transform (FFT), short time Fourier transform (STFT) etc. have been used to localize the exact AE source in different kinds of thin isotropic plates and composite plates (Eaton et al. 2012; Zhi et al. 2014; Suzuki et al. 1996; Jiao et al. 2004). Using these techniques, there is a possibility of having noise in the signal which may cause subsequent error in the obtained results. Such limitations can be overcome by the method of Wavelet Transform (WT) which analyses the AE displacement responses in time-frequency domain. According to the study, it was found that the method of WT is very suitable technique in investigating the frequency components of an experimentally obtained AE signal as a function of time and in splitting valid or effective signals from the noise (Shiotani 2006). Another study shows that there exists a relationship between group velocity and frequency. The group velocity is defined as the property of the material and at different frequencies its value will be different. Moreover, for different modes (A0, S0, A1, S1 etc.) these curves will be different. The time of arrival for these modes can be determined using this approach and also the source can be localized (Breckenridge et al. 1990).

From the above, it is found that most of the existing research work related to AE source localization using signal processing-based approaches involve thin plates of isotropic material and laminated composites. However, similar studies on RC slabs, which can be considered as moderately thick and anisotropic in nature, are rare. Hence, in the present paper, an attempt has been made to find the effectiveness of using WT technique for determination of AE source in a laboratory scale RC slab experimentally. For this purpose, signals obtained at a single AE sensor for different locations of RC slab of simulated AE source is used.

2 Methodology

The test was performed in the laboratory using a RC slab. The dimension of the slab is $1200 \times 750 \times 40$ mm^3 with 6 mm re-bars and M20 grade of concrete were used

to prepare the sample. In the laboratory, using the AE set up, the test was conducted. For the capturing of AE signals, R6D sensor was used. It has a very good sensitivity property and frequency response for the range of 35–100 kHz. The sensor was placed at the center of the slab (Fig. 1(a)) and the damage/defect is simulated by pencil lead break which causes AE source. These sensors are used to capture the location details of the simulated damage source. Each of the points of lead break are 5 cm apart from each other. The pencil lead breaks or PLB are generally used for producing simulated damage source, which are well-known as the Hsu-Nielsen (H-N) source (Breckenridge et al. 1990). A mechanical lead-pencil lead of 0.5 mm thickness is pressed gently against the upper surface of the slab till the lead breaks. The surface of the structure deforms in the nearby locations because of the pressure applied through pencil-lead. It causes the release of sudden and accumulated stress, which are called as the acoustic waves. These waves are in general, regarded as the surface waves, received with AE sensors which are placed in the similar plane. The AE-sensors transform these subsequent acoustic waves to resulting AE signals. Thereafter, the AE pre-amplifiers are generally used for the amplification of the signals and by using the filters, the removal of system noises is completed in the processor, where the data is acquired. This process helps to convert the AE signal into distinguishable form for the users (Fig. 1(b)). All the AE responses were recorded and further investigated using the AGU-Vallen Wavelet, the commercially available software for WT analysis (web site www.vallen.de).

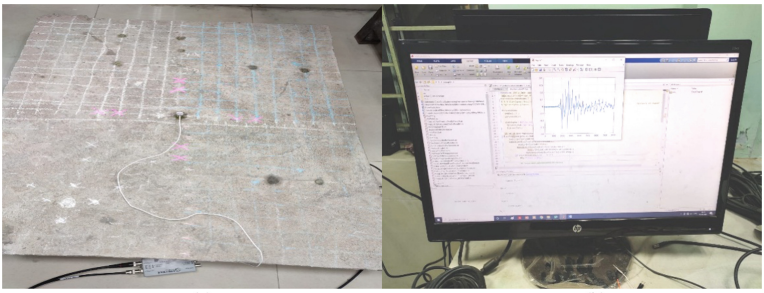

(a) (b)

Fig. 1. Experimental set-up; (a) Sensor placed in the centre of the slab, (b) Acquired data through AE system.

2.1 Wavelet Transform

The continuous Wavelet Transform of function *f(t)* is defined as:

$$Wf(b,a) = \frac{1}{\sqrt{a}} \int_{-\infty}^{\infty} f(t) \overline{\psi\left(\frac{t-b}{a}\right)} dt \tag{1}$$

where a > 0 and the overbar indicates the complex conjugate (Chui, 1992). The function $\psi(t)$ is termed as the analyzing wavelet. It fulfills the acceptability condition as below:

$$\int_{-\infty}^{\infty} \frac{\left|\hat{\psi}(\omega)\right|^2}{|\omega|} d\omega < \infty \tag{2}$$

where, $\hat{\psi}(\omega)$ represents the Fourier transform of $\psi(t)$. Although any wavelets satisfying the permissibility condition can be chosen, Gabor wavelet is well-known for providing the finest time-frequency solution (Jeong and Jang, 2000). The Gabor function is expressed as:

$$\psi_g(t) = \frac{1}{\sqrt[4]{\pi}} \sqrt{\frac{\omega_0}{\gamma}} exp\left[-\frac{\left(\frac{\omega_0}{\gamma}\right)^2}{2} t^2 \right] \exp(i\omega_0 t) \tag{3}$$

And, its Fourier Transform is

$$\hat{\psi}_g(\omega) = \frac{\sqrt{2\pi}}{\sqrt[4]{\pi}} \sqrt{\frac{\gamma}{\omega_0}} exp\left[-\frac{\left(\frac{\gamma}{\omega_0}\right)^2}{2} (\omega - \omega_0)^2 \right] \tag{4}$$

where, ω_0 and γ are the positive constants. The Gabor function may well be measured as a Gaussian window function centered at $t = 0$ and its Fourier transform centered at $\omega = \omega_0$. The function $\psi_g\left(\frac{t-b}{a}\right)$ is then centered on $t = b$ and its Fourier transform is centered about $\omega = \frac{\omega_0}{a}$. The WT *Wf(a,b)* using Gabor wavelet therefore denotes the time-frequency component of *f(t)* around $t = b$ and $\omega = \frac{\omega_0}{a}$.

2.2 Time Frequency Analysis

For the analysis in the time-frequency domain of dispersive waveforms, two harmonic waves of slightly different frequencies ω_1 *and* ω_2 and of equal unit amplitudes are considered. It is assumed that the waves are propagating in the x direction. Hence,

$$u(x, t) = e^{-i(k_1 x - \omega_1 t)} + e^{-i(k_2 x - \omega_2 t)} \tag{5}$$

If $\frac{k_1+k_2}{2} = k_c$; $\frac{\omega_1+\omega_2}{2} = \omega_c$; $\frac{k_1-k_2}{2} = \Delta k$ *and* $\frac{\omega_1-\omega_2}{2} = \Delta\omega$ *then:*

$$u(x, t) = 2cos(\Delta k x - \Delta\omega x) e^{-i(k_c x - \omega_c t)} \tag{6}$$

From the above equation it can be understood that the resulting wave is having two portions:

1. The carrier wave represented by the exponential part. This travels with a phase velocity $c_p = \frac{\omega_c}{k_c}$
2. The modulated wave represented by cosine term moves with the group velocity $c_g = \frac{d\omega}{dk}$ while $\Delta k \to 0$

When we use the Gabor wavelet as investigating wavelet, the WT of *u (x,t)* is given by:

$$W_u(x, a, b) = \sqrt{a}\left\{e^{-i(k_1 x - \omega_1 b)}\overline{\hat{\psi}_g(a\omega_1)} + e^{-i(k_2 x - \omega_2 b)}\overline{\hat{\psi}_g(a\omega_2)}\right\} \tag{7}$$

Hence the magnitude of WT can be obtained as:

$$|W_u(x, a, b)| \approx \sqrt{2a}\left|\hat{\psi}_g(a\omega_c)\right|[1 + \cos(2\Delta k x - 2\Delta\omega b]^{1/2} \tag{8}$$

where, it is assumed that $\Delta\omega$ is adequately small such that:

$$\hat{\psi}_g(a\omega_1) \approx \hat{\psi}_g(a\omega_2) \approx \hat{\psi}_g(a\omega_c)$$

From the above it can be seen that the WT magnitude becomes maximum when:

$$\Delta k x = \Delta\omega b \; or \; b = \frac{\Delta k}{\Delta\omega} x \; or \; b = \frac{x}{c_g} \; and \; a = \frac{\omega_0}{\omega_c}$$

Thus, it can be understood that the position of the peak on the (a, b) plane specifies the time of arrival of the group velocity c_g at frequency $\omega_c = \frac{\omega_0}{a}$. If $\omega_0 = 2\pi$ then $\omega_c = \frac{2\pi}{a} = 2\pi f$ where $f = \frac{1}{a}$.

From the above formulation as discussed in Sect. 2.1 and 2.2, it can be observed that there exists a relationship between the group velocity and the frequency at which the peak value for WT occurs. The group velocity is the property of the material and for different frequency values, its value will be different. Moreover, for different modes (both anti-symmetric and symmetric) these curves will be different. Thus, for a particular material, frequency-group velocity relations can be obtained relevant to particular modes. On the other hand, the frequency at which the peak value for WT occurs can be obtained by wavelet transform of the flexural mode AE waveforms at time domain. Thus, the time-frequency relation for the AE waveforms may be obtained using WT. From this relation the frequency and the corresponding time at which the maximum magnitude of WT is occurring are obtained. From the frequency-group velocity relation the group velocity corresponding to such frequency values are found. This group velocity multiplied with the time gives the travel distance which will show the position of the AE source.

3 Results and Discussion

The WT is applied on the experimentally obtained data and the time-frequency relation will be obtained containing different WT magnitudes at different time and frequency. Moreover, using such time-frequency domain data, AE source can be localised using the group velocity. The dispersion curves are drawn. For reinforced concrete the P-Wave and S-Wave velocity considered are 3400 m/s and 2200 m/s (Mirgal et al. 2020) and the thickness of the sample is 40 mm. In the dispersion curve setup screen, the option for "Show Curves" can be found. Here the "A0, A1, S0 and S1 modes" option is chosen (Fig. 2). The response data at 15 cm & 20 cm distance on different directions from the source is used for WT using the default parameters of the AGU Vallen Wavelet (Fig. 3).

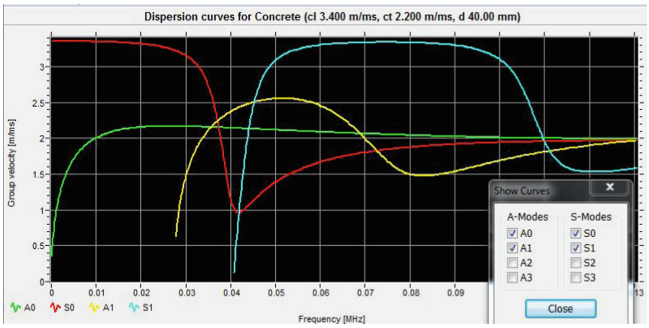

Fig. 2. Dispersion curves for concrete slab of 40 mm thickness (P-Wave Velocity 3400 m/sec and S-Wave Velocity 2200 m/sec).

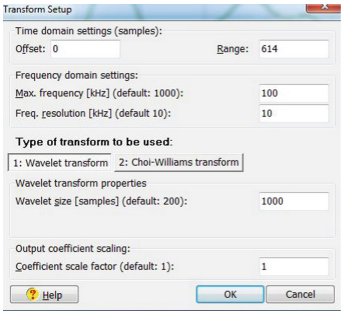

Fig. 3. Wavelet setup screen for AGU Vallen Wavelet.

The 2D colour contour diagram for WT coefficients are plotted. The colour scale is a linear scale with red colour indicating the greatest magnitude region of the WT. On the other hand, the pink colour is signifying the smallest or zero-magnitude region. On the same WT diagram the group velocity curve obtained is imported by choosing the distance. For the study specimen, it is observed that the fundamental symmetric and

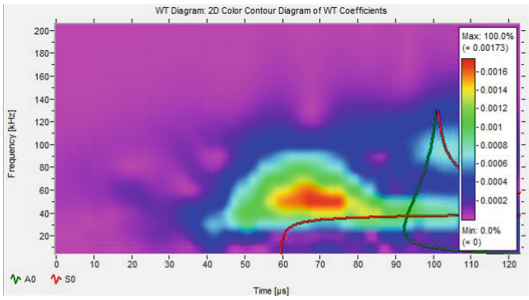

Fig. 4. WT for flexural AE response due to simulated AE source with superimposed fundamental anti-symmetric (A0) and symmetric (S0) modes after converting group velocity to time based on 15 cm distance of propagation.

anti-symmetric modes (S0 and A0) were not passing through the highest magnitude of the WT contour diagram (Fig. 4), whereas higher symmetric (S1) and anti-symmetric (A1) mode touch the regions corresponding to highest magnitude (Fig. 5 and 6) for different distance of the lead-break.

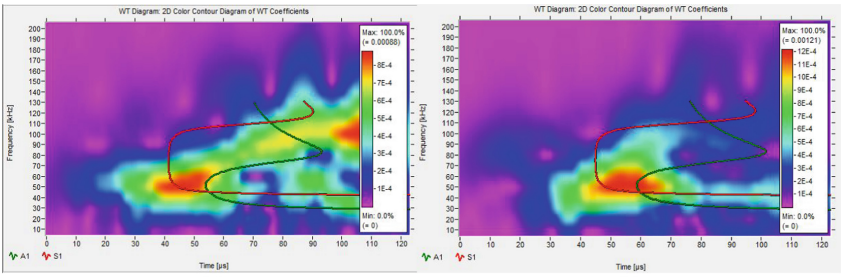

(a) (b)

Fig. 5. 2D colour contour diagram for WT coefficients for concrete slab for the location 15 cm away from source in (a) lateral direction, (b) longitudinal direction.

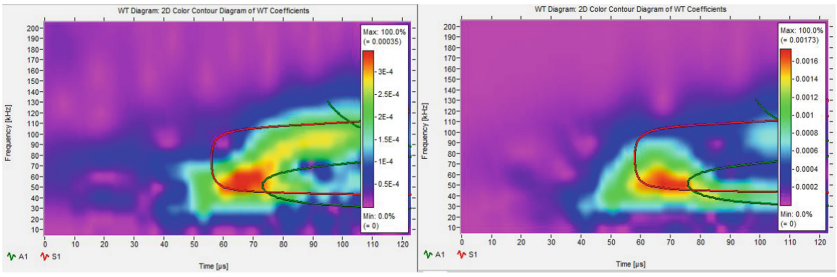

(a) (b)

Fig. 6. 2D colour contour diagram for WT coefficients for concrete slab for the location 20 cm away from source in (a) lateral direction, (b) longitudinal direction.

Table 1 gives the details about the maximum WT coefficients, corresponding group velocity, time at which the maximum WT coefficients are obtained. The distance between the source and the damage location is calculated by multiplying the time at which the maximum WT co-efficient obtained and group velocity. The results show that for the distance from source of 15 cm, the identified distance from the response point to the source using the group velocity of higher symmetric and anti-symmetric modes S1 and A1 are 14.94 cm and 15.14 cm respectively. From these, it could be stated that the identified distance from the response point to the source using the group velocity are in near vicinity to the exact distance. The percentage of error are 0.4% and 0.93% for S1 mode and A1 mode respectively. For the distance from source of 20 cm, similar kind of observations are found as the identified distance are 20.05 cm and 20.33 cm for S1 and A1 mode respectively. The corresponding errors are 0.25% and 1.65% respectively. This indicates that for the RC sample, the higher symmetric mode (S1) of group velocity curve comparatively predicts the location of damage better than the higher anti-symmetric mode (A1).

Table 1. Maximum WT coefficients corresponding to frequency, group velocity and calculated distance from source for test sample

Distance from source (cm)	Mode	Time at which Max WT coefficient obtained (micro sec)	Group velocity (m/ms)	Distance identified (Group Velocity x Time) (cm)	Error (%) in terms of distance from source	Maximum WT coefficient
15	S1	46.71	3.2	14.94	0.4	0.001286
	A1	58.69	2.58	15.14	0.93	0.001152
20	S1	60.39	3.32	20.05	0.25	0.001452
	A1	78.2	2.6	20.33	1.65	0.001351

4 Concluding Remarks

The presence of higher modes of group velocity curves prove that for thick RC slabs, the higher modes are predominant. For RC slab, the WT analysis of AE waveform in time-frequency domain, the fundamental modes of group velocity cannot predict the source of damage since the group velocity curves are not passing through the region corresponding to highest magnitude of WT diagram. On the other hand, the results showed that the higher modes like S1, A1 can predict the same with better accuracy as these curves are passing through the region corresponding to highest magnitude of WT diagram. Among the higher modes of group velocity, the higher symmetric mode (S1) mode gives the better result with a very small error than the anti-symmetric mode i.e. the S1 mode show better accuracy to localize the damage. These results confirm that the studies conducted with small-scale RC specimens, there is a great potential of using wavelet analysis for detection of damage of concrete structures with better accuracy. With more correctness in the casting of the sample, with different samples of different dimensions, the test could be performed to show better results.

References

Breckenridge, F.R., et al.: Transient sources for acoustic emission work. In: Yamaguchi, K. et al. (eds.) Progress in Acoustic Emission, JSNDI, Tokyo, vol. 1990, pp. 20–37 (1990)

Chen, Z., Li, D., Li, Y., Feng, Q.: Damage analysis of FRP/Steel composite plates using acoustic emission. Pac. Sci. Rev. **16**(3), 193–200 (2014). https://doi.org/10.1016/j.pscr.2015.03.002

Chui, C.K.: An Introduction to Wavelets. Academic Press, San Diego (1992)

Eaton, M.J., Pullin, R., Holford, K.M.: Acoustic emission source location in composite materials using delta T mapping. Compos. Part A: Appl. Sci. Manuf. **43**(6), 856–863 (2012). https://doi.org/10.1016/j.compositesa.2012.01.023

Ebrahimkhanlou, A., Salamone, S.: Acoustic emission source localization in thin metallic plates: a single-sensor approach based on multimodal edge reflections. Ultrasonics **78**, 134–145 (2017). https://doi.org/10.1016/j.ultras.2017.03.006

Jeong, H., Jang, Young-Su.: Wavelet analysis of plate wave propagation in composite laminates. Compos. Struct. **49**(4), 443–450 (2000). https://doi.org/10.1016/S0263-8223(00)00079-9

Jiao, J., et al.: Application of wavelet transform on modal acoustic emission source location in thin plates with one sensor. Int. J. Pressure Vessels Piping **81**(5), 427–431 (2004). https://doi.org/10.1016/j.ijpvp.2004.03.009

Mirgal, P., Pal, J., Banerjee, S.: Online acoustic emission source localization in concrete structures using iterative and evolutionary algorithms. Ultrasonics **108**, 106211 (2020). https://doi.org/10.1016/j.ultras.2020.106211

Naderpour, H., Ezzodin, A., Kheyroddin, A., Amiri, G.G.: Signal processing based damage detection of concrete bridge piers subjected to consequent excitations. J. Vibroeng. **19**(3), 2080–2089 (2017). https://doi.org/10.21595/jve.2015.16474

Panjsetooni, A., Bunnori, N.M., Vakili, A.H.: Damage source identification of reinforced concrete structure using acoustic emission technique. Sci. World J. **2013** (2013). https://doi.org/10.1155/8086

Sengupta, S., Datta, A., Topdar, P.: Structural damage localisation by acoustic emission technique: a state of the art review. Latin Am. J. Solids Struct. **12**(8), 1565–1582 (2015). https://doi.org/10.1590/1679-78251722

Shiotani, T.: Evaluation of repair effect for deteriorated concrete piers of intake dam using AE activity. Adv. Mater. Res. **13**, 175–180 (2006). https://doi.org/10.4028/www.scientific.net/AMR.13-14.175

Suzuki, H., et al.: Wavelet transform of acoustic emission signals. J. Acoust. Emission **14**(2), 69–84 (1996)